Heterogeneous & Homogeneous & Bio- & Nano-

CHEMCATCHEM

CATALYSIS

Accepted Article

Title: Effect of promoter nature on synthesis gas conversion to alcohols over (K)MeMoS2/Al2O3 catalysts

Authors: Vladimir V. Maximov, Eugenii A. Permyakov, Viktor S. Dorokhov, Anjie Wang, Patricia J. Kooyman, and Victor M. Kogan

To be cited as: *ChemCatChem* 10.1002/cctc.201901698

Link to VoR: http://dx.doi.org/10.1002/cctc.201901698

A Journal of ChemPubSoc Europe

WILEY-VCH

www.chemcatchem.org

ChemCatChem

Effect of promoter nature on synthesis gas conversion to alcohols over (K)MeMoS2/Al2O3 catalysts

--Manuscript Draft--

Manuscript Number:	cctc.201901698R2
Article Type:	Full Paper
Corresponding Author:	Victor M. Kogan, Ph.D., D. Sc., Prof. Moscow, RUSSIAN FEDERATION
Corresponding Author E-Mail:	vmk@ioc.ac.ru
Order of Authors (with Contributor Roles):	Vladimir V. Maximov, Ph.D. student
	Eugenii A. Permyakov
	Viktor S. Dorokhov
	Anjie Wang
	Patricia J. Kooyman
	Victor M. Kogan, Ph.D., D. Sc., Prof. (Conceptualization: Lead; Project administration: Lead; Supervision: Lead; Writing – review & editing: Lead)
Keywords:	Higher alcohol synthesis * Synthesis gas conversion * K-modified MeMoS2 catalysts * FeMoS2 * CoMoS2 * NiMoS2
Abstract:	The influence of the promoter nature and of a modifier in (K)(Me)MoS2/Al2O3 (Me = Fe, Co, Ni) catalysts on the conversion and selectivity of products of synthesis gas conversion to alcohols and other oxygenates was investigated. Relationships between promoter nature, hydrocarbon chain length and selectivity in the formed alcohols were established. Electronic structure of a promoter atom in an active site (AS) was found to strongly affect selectivity of alcohol formation. Promotion of the S-edge by Fe, Co or Ni suppressed hydrogen activation, which resulted in a lower synthesis gas conversion. Promotion of the M-edge by Fe, Co, or Ni entailed the formation of double vacancies which are active sites of synthesis gas conversion. Potassium affected the oxophilicity of Mo atoms and reduced Co/Ni-promoted MoS AS. It decreased the probability of C-O bond breaking in the adsorbed intermediate and shifted selectivity from the formation of alkyl towards alkoxide fragments over these catalysts.
Response to Reviewers:	REVIEWER REPORT EVALUATION: Reviewer's Responses to Questions 1. Please rate the importance of the revised manuscript Reviewer #1: Important (top 35%) 2. Please rate the length of the revised manuscript Reviewer #1: Concise 3. Are further changes/additions required Reviewer #1: No

	4. Please indicate which other journal you consider more appropriate Reviewer #1: (No Response) COMMENTS TO AUTHOR: ******** Reviewer 1: Comments have considered and modifications applied to the new manuscript. the new submission is fine for me Editor's Comments: Please pay attention to the following when revising your manuscript: • Address information is missing or incomplete. - Please provide academic titles (e.g., Prof., Dr., or Prof. Dr.) for all authors. • A Table of Contents entry has not yet been provided. Please provide an appropriate text (60-80 words) and a color graphic (5.5 cm wide x 5 cm tall OR 11.5 cm wide x 2.5 cm tall) in your final revision.
Section/Category:	French Conference on Catalysis 2
Additional Information:	
Question	**Response**
Submitted solely to this journal?	Yes
Has there been a previous version?	No
Do you or any of your co-authors have a conflict of interest to declare?	No. The authors declare no conflict of interest.
Animal/tissue experiments?	No
Do you or any of your co-authors have a conflict of interest to declare?	No
Does the research described in this manuscript include animal experiments or human subjects or tissue samples from human subjects?	No

ChemCatChem
10.1002/cctc.201901698

Effect of promoter nature on synthesis gas conversion to alcohols over (K)MeMoS$_2$/Al$_2$O$_3$ catalysts

List of authors

Name	Title	Affiliation	E-mail
V.V. Maximov	Ph.D student	N.D. Zelinsky Institute of Organic Chemistry, Russian Academy of Sciences, 47 Leninsky prospect, Moscow 119991, Russia	maximovzioc@gmail.com
E.A. Permyakov	Researcher	N.D. Zelinsky Institute of Organic Chemistry, Russian Academy of Sciences, 47 Leninsky prospect, Moscow 119991, Russia	permeakra@gmail.com
V.S. Dorokhov	Dr.	N.D. Zelinsky Institute of Organic Chemistry, Russian Academy of Sciences, 47 Leninsky prospect, Moscow 119991, Russia	viktor.s.dorokhov@yandex.ru
A. Wang	Prof.	State Key Laboratory of Fine Chemicals, School of Chemical Engineering, Dalian University of Technology, Dalian 116024, China	ajwang@dlut.edu.cn
P.J. Kooyman	Prof.	ChemEng, University of Cape Town, Private Bag X3, Rondebosch 7701, South Africa	patricia.kooyman@uct.ac.za
V.M. Kogan	Prof.	N.D. Zelinsky Institute of Organic Chemistry, Russian Academy of Sciences, 47 Leninsky prospect, Moscow 119991, Russia	vmk@ioc.ac.ru

10.1002/cctc.201901698

Appropriate text and color graphic:

Effects of promoter and of a modifier of (K)(Me)MoS_2/Al_2O_3 (Me = Fe, Co, Ni) catalysts on syngas conversion into alcohols and their selectivity have been investigated. Relationships between promoter nature, hydrocarbon chain length and selectivity in the formed alcohols were established. Electronic structure of a promoter atom in an active site was found to strongly affect selectivity of alcohol formation. Potassium affected oxophilicity of Mo atoms and reduced Co/Ni-promoted MoS active sites.

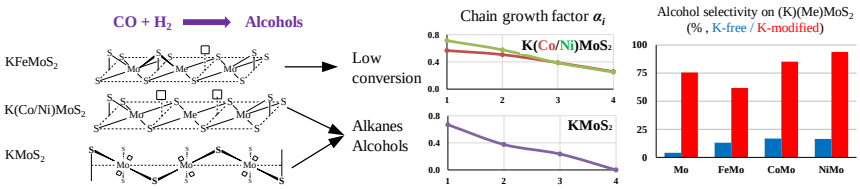

10.1002/cctc.201901698

Table of contents

10.1002/cctc.201901698

Effect of promoter nature on synthesis gas conversion to alcohols over (K)MeMoS$_2$/Al$_2$O$_3$ catalysts

V.V. Maximov[1], E.A. Permyakov[1], V.S. Dorokhov[1], A. Wang[2], P.J. Kooyman[3], and V.M. Kogan[1*]

[*]vmk@ioc.ac.ru

[1]N.D. Zelinsky Institute of Organic Chemistry, Russian Academy of Sciences, 47 Leninsky prospect, Moscow 119991, Russia
[2]State Key Laboratory of Fine Chemicals, School of Chemical Engineering, Dalian University of Technology, Dalian 116024, China
[3]ChemEng, University of Cape Town, Private Bag X3, Rondebosch 7701, South Africa

Abstract

The influence of the promoter nature and of a modifier in (K)(Me)MoS$_2$/Al$_2$O$_3$ (Me = Fe, Co, Ni) catalysts on the conversion and selectivity of products of synthesis gas conversion to alcohols and other oxygenates was investigated. Relationships between promoter nature, hydrocarbon chain length and selectivity in the formed alcohols were established. Electronic structure of a promoter atom in an active site (AS) was found to strongly affect selectivity of alcohol formation. Promotion of the S-edge by Fe, Co or Ni suppressed hydrogen activation, which resulted in a lower synthesis gas conversion. Promotion of the M-edge by Fe, Co, or Ni entailed the formation of double vacancies which are active sites of synthesis gas conversion. Potassium affected the oxophilicity of Mo atoms and reduced Co/Ni-promoted MoS AS. It decreased the probability of C-O bond breaking in the adsorbed intermediate and shifted selectivity from the formation of alkyl towards alkoxide fragments over these catalysts.

1. Introduction

Growth in global demand for major energy sources, including liquid fuels, requires a revision of the world energy consumption structure. Today, 96% of liquid fuels is produced from petroleum. Liquid fuel production processes from coal (coal-to-liquids, CTL) and light hydrocarbons (gas-to-liquids, GTL) have been the focus of R&D since the beginning of the 20th century.[1] Nonetheless, these processes have not found extensive applications so far and cannot compete with liquid fuels produced from crude oil.

CTL and GTL processes usually proceed *via* intermediate production of synthesis gas. Synthesis gas can be sourced from natural and associated gas, coal, other combustible minerals, and biomass.[2,3] Synthesis gas is a very convenient intermediate for the synthesis of petrochemicals and can yield long-chain linear

alkanes and terminal alkenes, fatty alcohols, aldehydes, carboxylic acids, and other oxygenates.[1] Alcohols like ethanol and methanol can be used to increase octane rating of gasoline in particular. Higher alcohols are more favorable as fuel additives than methanol because of their lower volatility and better solubility in hydrocarbons (HC). In the environmental context, higher alcohols are preferable because they reduce the amount of soot particles, carbon, and nitrogen oxides in exhaust gases. Furthermore, higher alcohols are widely used as precursors in petrochemistry and medical chemistry.[4,5]

Review[4] describes various methods for the preparation of higher alcohols such as fermentation of sugars, synthesis and subsequent carbonylation of methanol, methanol cross-coupling with CO, etc. In terms of future applications, of most interest is a direct synthesis of higher alcohols from synthesis gas over Rh, Cu, Co, and Fe catalysts. However, a majority of metal and oxide catalysts has a significant drawback – they are susceptible to poisoning with sulfur-containing compounds, even if the latter are present in raw materials in trace quantities (ppm). Sulfides of transition metals do not have this disadvantage and, moreover, their catalytic activity is comparable to or higher than that of metal and oxide catalysts.[6]

Various (Me)MoS_2-based catalysts can be used for catalytic synthesis gas conversion.[7–10] A high content of sulfidic impurities in the feedstock (50-100 ppm H_2S) helps inhibits sulfur removal from these catalysts, preventing deactivation and extending catalyst life.[11,12] Sulfide catalysts are more resistant to carbon deposition, than conventionally applied oxide ZnCu and ZnCr catalysts.[12] Catalysts based on transition metal sulfides are tolerant to the presence of sulfur in the feedstock and can improve performance of industrial processes for catalytic synthesis gas conversion to alcohols.

Catalysts based on potassium-modified molybdenum disulfide for the production of alcohols from synthesis gas were introduced by Dow Chemical Company and Union Carbide Corporation in the mid-1980s.[13,14] A special feature of these catalysts is that a mixture of methanol, C_{2+} alcohols and hydrocarbons is formed in the course of synthesis gas conversion. The products are mainly primary linear alcohols.

Catalysis occurs mainly on coordinative unsaturated sites (CUS) formed on the edges of (Co/Ni)MoS_2 catalysts.[10,15–22] Co and Ni promoter atoms located on the MoS_2 crystallite edges participate in the CUS formation.[11,12,22-25] Addition of potassium to the (Co/Ni)MoS_2 system reduces metal atoms and increases the MoS_2 slab length and stacking degree.[22,26-28] In hydrodesulfurization reactions, this induces a decrease in catalytic activity and a shift in selectivity from hydrogenation to hydrodesulfurization.

Computer simulation of MoS CUS in (K)(Me)MoS (Me = Fe, Co, Ni, collectively referred to as promoters in this study) showed that Lewis acidity of the promoter atom and affinity for sulfur decreased in the order Fe>Co>Ni. Addition of potassium (referred to as a modifier) increased the Me-S bond strength and decreased the number of vacancies for MoS and FeMoS, but not for CoMoS and

NiMoS. On the other hand, addition of potassium increased the Me-H bond strength facilitating H_2 activation.[22,29]

In this study, we report experimental results regarding the influence of the promoter metal nature both in the presence and in the absence of potassium (modifier) on the catalytic activity of (K)(Me)MoS_2 (Me = Fe, Co, Ni) samples in synthesis gas conversion to higher alcohols and/or hydrocarbons and on the carbon chain size of the products. The results are discussed using previously obtained DFT computational data on the electronic structure and on the affinity of model active sites for sulfur, CO, and hydrogen.[22]

2. Experimental

2.1. Preparation of materials and catalysts

Textural characteristics of the γ-Al_2O_3 support material are listed in Table 1.

To study the effect of ***d***-metals (Fe, Co and Ni) and potassium on the catalytic performance of MoS_2, catalysts of different composition were prepared and evaluated. As a r=Me/(Me+Mo) molar ratio (promotion degree, Table 2) of 0.3 previously provided maximum promotion of molybdenum disulfide edges as well as the highest alcohol yield.[24-28] Promotion degree r ≈ 0.3 was used in this study. The composition of the catalysts was determined using XRF (see Section 2.2.2 and Table 2).

The catalysts were prepared *via* wet impregnation. A typical preparation procedure for solution impregnation is:

0.48 g (5 mmol) of ammonium heptamolybdate (Alfa Aesar, tetrahydrate, chemically pure 99%) was dissolved in a mixture of 1.5 ml of distilled water and 1 ml of 20% NH_4OH solution before 0.40 g (10 mmol) of KOH (analytical grade, 98%) was added. This solution 1 was added to solution 2 of Me acetate (Me=Fe^{3+}, Co^{2+}, Ni^{2+}) (Alfa Aesar, tetrahydrate, chemically pure 98%) (2.5 mmol) and 1.05 g (5 mmol) of citric acid in 1 ml of distilled water. Al_2O_3 (3 g) was impregnated with resulting solution 3 following by drying on air for 2 hours at 60°C and then for 5 hours at 100-110°C.

2.2. Physical characteristics of supports and catalysts

2.2.1. Textural characteristics of the samples

Textural characteristics were determined from N_2 adsorption and desorption isotherms measured using an ASAP 2020 Plus instrument (Micromeritics, USA) at 77 K. Before degassing, oxide samples were kept under argon flow for 3 hours and sulfide samples were kept under hydrogen flow for 3 hours. The oxide samples

were degassed at 110°C for 4 h at 10^{-4} mm Hg and the sulfide samples at 250°C for 4 h at 10^{-4} mm Hg.

The specific surface was determined using the BET equation. The total pore volume was determined at a relative pressure P/P_o = 0.99. The mesopores size distribution was calculated from the desorption branch of the isotherm using the method of Barrett, Joyner and Halenda (BJH).[30] The cumulative pore volume during desorption, according to the BJH method, was taken as the mesopore volume (considering the adsorption film thickness on the mesopore surface). The micropore volume in the samples was determined using the t-plot method[31] and by comparing the total pore and mesopore volumes.

Gas sorption analysis was performed according to standard procedures. All sample cells were calibrated before use. Approximately 0.1 g of any given sample was taken for analysis. Analysis was programmed to obtain at least 25 points on the adsorption curve (with 10 points in the 0.01-0.30 p/p_o region for BET and 6 points between 0.3-0.6 p/p_o for t-plot/α-S) and 45 points on the desorption curve for BJH. Some samples were checked for reproducibility and the error was found to be less than 5%. The obtained specific surface, volume and pore size values are summarized in Table 1.

2.2.2. Elemental composition characterization

The elemental composition of the catalysts was determined using an EDX-7000 X-ray fluorescence spectrometer (Shimadzu); tube anode – Rh, tube current 8–200 mA, voltage 15–50 kV. All samples were crushed before measurements. The error of the XRF method was found to be ± 1 wt.%. The spectra were processed using the method of fundamental parameters.[32] The elemental composition data are given in Table 2.

2.3. Catalytic experiments and analysis of products

Before catalytic experiments, the samples were sulfided in an autoclave using elemental sulfur under the following conditions: temperature 360 °C and hydrogen pressure 60 atm (*catalyst:sulfur weight ratio = 5:1*) during 1 hour. After sulfiding, the samples were placed in the catalytic reactor under inert atmosphere.

Synthesis gas conversion was carried out in a fixed-bed flow reactor using 3 g of the catalyst, P = 5 MPa, T = 300-360 °C, mass feed rate 760 $l\ h^{-1}\ (g\ cat)^{-1}$, feed gas composition $CO:H_2:Ar$=45%:45%:10%. Argon was used as an internal standard for gas chromatography (GC).

The gas products were analyzed using an LHM-80 GC with a thermal conductivity detector and two one-meter packed columns (molecular sieves CaA (Ar, CH_4, CO) and Porapak Q (CO_2, C_{2+})). The liquid products (alcohols, aldehydes, esters, etc.) were analyzed using a Crystal-2000M GC with a flame

ionization detector and a 50-meter HP-FFAP capillary column. Carrier gas was high purity helium for both GCs.

The synthesis gas conversion results are given for the carbon atom. Data on the elemental composition of the catalysts were used to calculate specific conversion (activity per mmole of Mo) of synthesis gas X_C^{Mo} (Table 2) according to Eq 1 and 2:

$$X_C = 1 - \frac{n_{CO}^{After\ reaction}}{n_{CO}^{In\ feed}} \quad (1)$$

$$X_C^{Mo} = \frac{X_C}{\vartheta_{Mo}} \quad (2)$$

where X_C – synthesis gas conversion; X_C^{Mo}- specific synthesis gas conversion; n_{CO}^{feed} and $n_{CO}^{Afterreaction}$ – CO content, in mmol, in initial synthesis gas and in the products, respectively; ϑ_{Mo} - molybdenum content, in mmol, in the corresponding sample.

It is commonly accepted[13,33-35] that selectivity in this reaction is calculated in CO_2 free basis approximation. The reason for that is the following: the CO_2 is mainly formed in the course of water gas shift or Boudouard reactions and is considered as by-product does not affecting the selectivity of the target products. That is why we excluded CO_2 from selectivity balance calculations. CO_2-free selectivity was calculated using Eq. 3:

$$S_i^{CO_2-free} = \frac{S_i}{1 - S_{CO_2}}, \quad (3)$$

Where $S_i^{CO_2-free}$ — CO_2 free selectivity to *i* component; S_i – selectivity to *i* component; S_{CO_2} – CO_2 selectivity.

The carbon chain growth factor α_i was calculated using Eq. 4.

$$\alpha_i = \frac{\sum_{k>i} \frac{Y_k}{k}}{\sum_{k\geq i} \frac{Y_k}{k}}, \quad (4)$$

where α_i— chain growth factor for the intermediate with *i* carbon atoms; Y_k – yield of the component with the k number of carbon atoms.

The factor α_1 corresponds to the probability of the CO insertion to an intermediate containing one carbon atom with the formation of an intermediate with two carbon atoms; α_2 corresponds to the next step of CO addition to the intermediate with two carbon atoms to the intermediate with three carbon atoms, and so on.

3. Results

 10.1002/cctc.201901698

Specific surface, pore volume and particle size data for the molybdenum sulfide catalysts as well as for the bare alumina support are summarized in Table 1. The alumina support has a bimodal pore size distribution with maxima at 4.5 and 14.9 nm. Loading of the support material with the active phase reduces both the specific surface area and the pore volume. This effect was more pronounced for the potassium promoted catalysts. It should be noted that only minor part of potassium is intercalated, as for K_xMoS_2 intercalates only x~0.4 is achievable by more efficient process of direct intercalation of K(0) from dry liquid ammonia solution. The rest of potassium can either replace protons in Brønsted acidic sites on support or grab anion from environment during preparation, for example, forming (hydro) carbonates, obstructing small pores.

Elemental analysis data are presented in Table 2. The molybdenum content in the samples varies from 11 to 14% wt. The promotion degree ***r***=Me/(Mo+Me) [molar ratio] ranges from 0.22 to 0.30. The presence of potassium does not affect ***r***. The modification degree t= K/(Me+Mo) [molar ratio] ranges from 0.62 to 0.83.

The results of the catalytic experiments are summarized in Table 3 and considered in corresponding Figures 1-6. Figure 1 shows the specific conversion (per mmole Mo) of synthesis gas over the (Me)MoS_2 catalysts at temperatures between 300 and 360 °C at 50 atm. Addition of the promoter significantly reduces conversion as compared to that of non-promoted MoS_2. Of note is that nature of the promoter atom exerts a noticeable effect on the specific conversion value. Conversion decreased in the order of MoS_2>$FeMoS_2$>$CoMoS_2$>$NiMoS_2$. An increase in reaction temperature predictably increased synthesis gas conversion.

Figure 2 shows specific conversion of synthesis gas over the same samples, but modified with potassium. Potassium addition to MoS_2 and $FeMoS_2$ led to a decrease in conversion, whereas for $CoMoS_2$ and $NiMoS_2$ conversion increased upon potassium addition.

Addition of K did not affect the temperature dependence of the specific conversion for the (K)MoS_2, (K)$NiMoS_2$ and (K)$FeMoS_2$ samples. In the case of the $KCoMoS_2$ catalysts, the introduction of potassium essentially influenced the temperature dependence and an increase in synthesis gas conversion was observed (from 12.3% at 300 °C to 27.0% at 360°C).

Figures 3 and 4 show methane and C_{2+} hydrocarbon selectivity at T = 340 °C and p = 50 atm. Methane was the dominant product in the gas phase when the MoS_2 catalyst was utilized. In the case of $MeMoS_2$ (Me = Fe, Co, Ni), selectivity to C_{2+} hydrocarbons was higher than that to methane (Fig.3). Addition of promoters to molybdenum disulfide increased C_{2+} hydrocarbon selectivity (Fig. 4).

K-modification of the (Me)MoS_2 catalysts (Me = Fe, Co, Ni) suppressed hydrocarbon formation in favor of alcohols formation. The most pronounced reduction is observed for MoS_2 (from 50.5% to 11.5% for methane and from 45.5% to 13.0% for C_{2+}-hydrocarbons) and $FeMoS_2$ (from 63.1% to 16.7% for C_{2+}-hydrocarbons). The generation of C_{2+}-hydrocarbons (including alkenes) over $KCoMoS_2$ and $KNiMoS_2$ was almost completely suppressed. With temperature increasing methane and C_{2+} hydrocarbon yields increased for all samples.

The products of synthesis gas conversion over the molybdenum sulfide catalysts contained ethylene in small amounts (ethylene was found in larger amount on $MeMoS_2$, where Me = Fe, Co, Ni).

Selectivity to liquid products, including alcohols as major products and aldehides, ethers, esters, *etc*. as minor products (4% in sum), obtained on the $(K)(Me)MoS_2$ catalysts (Me = Fe, Co, Ni) at 340 °C and 50 atm. are depicted in Figures 5 and 6. Promotion by Fe, Co or Ni of K-free molybdenum disulfide did not affect the selectivity of the liquid products.

Modification of the $FeMoS_2$ catalyst with potassium did not bring about an increase in the liquid products yield. In the case of MoS_2, $CoMoS_2$ and $NiMoS_2$, potassium increased the liquid product yield approximately tenfold (Table 4). The yield of the liquid product over the $KFeMoS_2$ catalyst close to K-free sample (1.8% and 1.7% respectively).

Figure 6 shows selectivities for the individual products. It is seen that methanol was the main product for the $KMoS_2/Al_2O_3$ catalyst. No amyl alcohols were detected over non-promoted molybdenum disulfide. Co and Ni addition contribute to the increase in selectivity to C_{2+} alcohols. Maximum ethanol and propanol-1 selectivity is observed for the $KNiMoS_2/Al_2O_3$ catalyst.

Figure 7 shows dependences of the liquid product yield and efficiency of the potassium additive effect on the liquid products yield from the degree of molybdenum promotion by iron, nickel or cobalt. As seen from Figure 7, the values for the promoted catalysts are in a narrow region ***r*** – from 0.22 to 0.27, while the difference in these values is notable. This is indicative of a slight effect of the promotion degree in this range and, at the same time, of a significant effect of the promoter nature on the liquid products yield and of the difference in efficiency of the potassium effect on iron, cobalt and nickel, as promoting metals, in the composition of the MeMo-sulfide active site. The observed dependences testify to a stronger effect of potassium addition to the CoMoS site, a significant, though less strong, effect of its addition to NiMoS, and the lowest effect where it is added to the FeMoS site.

Figure 8 shows the dependence of the hydrocarbon chain growth factor α_i from the number of carbon atoms in the intermediate product on the $(Me)MoS_2$ catalysts. MoS_2 promotion by iron increased hydrocarbon chain growth factors α_1, α_2 and α_3. In the case of Co and Ni promoters, only α_1 increased, whereas α_2 was lower than that of the non-promoted sample and α_3 was zero. For all potassium-free samples, α_4 was zero.

Figure 9 shows the chain growth factors for the $K(Me)MoS_2$ catalysts. Modification with potassium dramatically increases the chain growth factor α_1 for the $KCoMoS_2$ and $KNiMoS_2$ catalysts. The influence of potassium on the MoS_2 catalyst is not significant. As for the Fe-containing catalyst, its modification with potassium substantially reduced the hydrocarbon chain growth factor α_1, whereas α_2, α_3 and α_4 were zero.

4. Discussion

According to,[19,22,36-39] activity of MoS_2-based catalysts is associated with the presence of CUS on the S- and M-edges. There is a significant number of vacancies on the S-edge of MoS_2 (Scheme 1a) in the thermodynamically stable state, whereas very few, if any, are present on the M-edge,[22] suggesting that the M-edge of the unpromoted catalyst does not exhibit activity in synthesis gas conversion. The DFT calculations show that adsorption of CO and dissociative adsorption of hydrogen can occur on the S-edge at (K)MoS sites with the formation of hydride hydrogen.[20,40,41] Reactions of hydride hydrogen with CO and other ligands are well known in metal complex chemistry. We believe that CO and other intermediate species are reduced by hydride hydrogen.

When MoS_2 is promoted with late ***d***-metals (Fe,Co,Ni and similar metals), a mixed MeMoS phase is formed. In this phase, promoter atoms substitute a part of molybdenum atoms on the crystallite edges.[4] Promotion of the S-edge by single Fe, Co or Ni atoms leads to the formation of (K)MeMoS sites that are not capable of activating hydrogen and thus are inactive in the CO hydrogenation reaction. Double sulfide vacancies (Scheme 1 b,c) form on the M-edge at MeMoS (Me = Fe, Co, Ni) and KMeMoS (Me = Co, Ni) sites, which can participate in synthesis gas conversion. We found that sulfur affinity of double vacancies on the M-edge of KFeMoS sites was much higher than for Co and Ni analogs.[22] All the (Me)MoS_2 catalysts show comparable activities. Addition of potassium completely inhibits activity only for the $FeMoS_2$ catalyst, slighly increases activity for the $MeMoS_2$, (Me=Co,Ni) catalysts and moderately decreases activity of MoS_2 catalyst. We suppose that activity of Fe,Co,Ni-promoted catalysts is defined by double vacancies and similar structures.

When the oxide form of the MoS_2 based catalyst is sulfided, potassium ions build a complex with the sulfide phase.[42] The nature of the complex was not established. Assumingly, potassium intercalates between MoS_2 crystallite layers.[43] Such intercalation is well known for bulk MoS_2 and results in the interlayer gap expansion according to XRD.[44] This increase was detected for a spent catalyst.[45] using XRD. However, TEM data do not show this increase in another study.[46]

The formation of vacancies on MeMoS sites on the M-edge and their properties can be understood using calculated formal oxidation states of edge atoms and determining corresponding electron states. By a formal electron count, metal atoms on the half-sulfided M-edge and at a single vacancy on the M-edge have oxidation numbers +4.66 and +3.66, respectively. These numbers are not typical for Fe-Ni. In double vacancies on MeMoS sites on the M-edge, the calculated oxidation state of the central atom is only +2.66, which is within the characteristic values for Fe and Co and occurs for Ni. Thus, double vacancies form fairly easily on these sites. However, since the +3 oxidation state is fairly common for Fe, the introduction of a small amount of electron density on the FeMoS slab is enough to stabilize single vacancies of KFeMoS sites on the M-edge.

In contrast, Ni in a double vacancy on the M-edge has the oxidation state +2.66, and the electron density donation can, at best, reduce it to the +2 oxidation state, which is characteristic for this metal. Furthermore, it is especially stable in

the square planar coordination which is highly common for metal atoms with the d^8 electron configuration. Further reduction is impeded because electrons then would have to go into the high-energy orbital $d_{x^2-y^2}$. In this state, the Ni atom only weakly binds the fifth ligand, if at all, and Mo atoms of the double vacancy of KNiMoS sites should bind CO stronger than Ni atoms of those sites. The high activity observed for the KNiMoS catalyst and its unusual temperature dependence of conversion suggest that its apparent conversion rate is limited by a process different from that in the other catalysts, probably due to greatly enhanced desorption.

In terms of properties, CoMoS sites on the M-edge rank between FeMoS and NiMoS. No sulfides of Co(III) are known. The closest compound is Co_3S_4 which at best can be described as mixed Co(II,III) sulfide. In contrast, Fe_2S_3 is known though it is not the most stable Fe sulfide. For this reason, KCoMoS sites on the M-edge exist in the form of active double vacancies under synthesis gas conversion conditions although their Lewis acidity is greatly reduced in comparison with CoMoS sites.

According to Ref.,[22] potassium modification of double vacancies of the M-edge of FeMoS sites results in the sulfur affinity increase (by the [vac][vac] + H_2S = H_2 + [vac][S] process) from ~0.7 eV to ~1.3 eV. Since the reaction energy

$$S_{surf} + H_2 = CUS_{surf} + H_2S$$

is below 1.2 eV, the process is thermodynamically feasible,[47-50] so double vacancies can form on FeMoS active sites on the M-edge though not on KFeMoS active sites. In contrast, we found that affinity to sulfur for (K)NiMoS sites on the M-edge was negative both for K-modified and K-free cases. CoMoS sites are somewhere between in terms of properties, exhibiting negative sulfur affinity for the CoMoS site and 0.8 eV for the KCoMoS site, still allowing the formation of double vacancies.

From this we can suppose that synthesis gas conversion over the (K)$MeMoS_2$ catalysts occurs on double vacancies on the M edge while the S-edge is not active. In contrast, synthesis gas conversion with the (K)MoS_2 catalyst is likely to occur on the S-edge. For the MoS_2 S-edge, each molybdenum atom has two coordination vacancies whereas vacancies of neighboring atoms group in pairs (Scheme 1a). Two coordination vacancies of one Mo atom on the 50% sulfided S-edge are separated by sulfur atoms. Thus, molecules or intermediates adsorbed on them are unlikely to interact with each other. On the other hand, each vacancy is close to a similar vacancy on one neighboring Mo atom and adsorbates on the two neighboring Mo-atoms can interact (Scheme 1bc). The qualitative distinction between the active sites related to (K)MoS_2 and (K)$MeMoS_2$ results in a difference in the chain growth factor between the (K)MoS_2 and (K)$MeMoS_2$ (Me=Co, Ni) catalysts.

Modification by potassium leads to an increase in synthesis gas conversion on both $KNiMoS_2$ and $KCoMoS_2$ catalysts. The increase in activity of $KNiMoS_2$ correlates with the increase in stability of the Mo-H bond on NiMoS sites on the M-edge shown in our earlier calculations.[22] The increased Mo-H bond energy is likely to imply an increased Mo-CH_3 bond energy. On the other hand, increased

activity of the $CoMoS_2$ catalyst correlates with the decrease in Mo-H and Co-CO bond energies. $KNiMoS_2$ has lower adsorption energies for CO and H as compared to $KCoMoS_2$, so we may conclude that the reaction rate in this case is determined by desorption or another reaction involving a Ni-X bond scission. Meanwhile the reaction rate on the K-free catalysts clearly correlates with bond energies and Lewis acidity of double vacancies on the M-edge. It should be noted that potassium addition almost completely suppresses the hydrocarbon formation on KCoMoS and the KNiMoS sites in favor of alcohol formation.

Selectivity to products of syngas conversion is determined by the rate of alkane elimination form alkyl intermediates and reactivity of aldehyde-type intermediate (Scheme 2). Reactivity of an aldehyde-type intermediate depends on polarization of C-O bond. Potassium addition to Mo-sulfide systems reduces metal atoms. It, in its turn, decreases probability of C-O bond cleavage in adsorbed intermediate on an active site and hinders reducing elimination of alkanes shifting selectivity from alkyl to alkoxide fragments.

Analysis of the synthesis gas conversion products on the $KCoMoS_2$/$KNiMoS_2$ catalysts shows measurable amounts of C_5 products with linear and branched chains. The chain growth factor (α) on $KCoMoS_2$ and $KNiMoS_2$ is much higher than on the other catalysts. Their high apparent activity is mostly due to greatly enhanced chain growth. A possible explanation is that, since potassium addition reduces metal atoms, it also leads to much higher nucleophilicity of alkyl and hydride intermediates which should greatly enhance the CO insertion rate even if CO is adsorbs only weakly. Hydrogenation/hydrodeoxygenation activity, on the other hand, is significantly lowered, leading to lower production of hydrocarbons.

The consistent and gradual decrease of α_i with increase of chain length was observed for all the studied catalysts. M-Alk bond reactivity toward the CO insertion is guarded by sterical factors. Thus, we can expect methyl and ethyl intermidiates have very different reactivity, but fairly similar for ethyl and *n*-propyl intermidiates, and even more so for n-propyl/n-butyl pair. On the other hand, CO insertion rate into primary (like ethyl) and secondary (like *i*-propyl) alkyl intermediates should be significantly different and, indeed, we found large amounts of branched products. Thus, the gradual decrease of α_i with increase of chain length can be attributed to sterical hindered CO-insertion of branched alkyl intermidiates

The branched products can form *via* isomerization of alkyl intermediates through alkene intermediates. Alkene formation by beta-elimination in alkyl intermediates has been well studied in organometallic chemistry and is known to be reversible. Addition of ethylene into synthesis gas leads to a marked increase in CO conversion, with formation of mostly C_3-products.[29] Scheme 3 shows equilibrium between *n*-propyl and *iso*-propyl fragments. Alcohols containing *iso*-propyl fragments were detected among other products (Fig. 6). The fraction of *iso*-products was higher over the $KCoMoS_2$ catalyst than over $KNiMoS_2$, i.e. isomerization of the alkyl fragment proceeded faster over the $KCoMoS_2$ catalyst.

Secondary alcohol formation cannot be explained by given mechanism because alcohol formation *via* the CO insertion can only produce primary alcohols.

This assumes co-elimination of alkyl- and aldehyde-type intermediates (Scheme 4). Coupling of C_2-fragments was earlier observed in ethanol conversion experiments with ^{13}C labels.[51]

At least two factors could cause low selectivity toward HC on the $KCoMoS_2/KNiMoS_2/KMoS_2$: potassium addition could stabilize alkyl intermediates, preventing desorption of alkanes, or the enhanced CO insertion rate could promote transformation of alkyl intermediates before they desorb. Suppression of the hydrodeoxygenation capability *per se* clearly does not play a role, because the CO bond scission is necessary for chain growth.

5. Conclusions

The influence of the promoter nature and the presence of potassium in the $(K)MeMoS_2/Al_2O_3$ catalysts on conversion and selectivity of the products of synthesis gas conversion to alcohols and other oxygenates was studied.

In synthesis gas conversion over the $MeMoS_2$ catalysts, the potassium additive is a promotor for $CoMoS_2$ and $NiMoS_2$, but an inhibitor for MoS_2 and especially for $FeMoS_2$.

Addition of potassium to molybdenum sulfide systems reduces metal atoms of the catalyst. Modification by potassium increases the CO molecule introduction into the metal-carbon bond of the surface alkyl intermediate. Potassium decreases oxophilicity of Mo atoms by reducing them.

The presence of secondary alcohols in the products indicates co-elimination of the carbon-containing intermediates. The presence of branched-chain products indicates isomerization of alkyl C_{4+} intermediates.

It has been supposed that synthesis gas conversion can occur either on the non-promoted S-edge of the $(K)MoS_2$ catalysts or on multiple vacancies on the M-edge of the $(K)MeMoS_2$ catalyst. Promotion of the S-edge by Fe, Co or Ni suppresses hydrogen activation, which results in lower synthesis gas conversion. Promotion of the M-edge by Fe, Co or Ni leads to the formation of double vacancies which are active sites of synthesis gas conversion.

Acknowledgement

The study was supported by the RFBR grant № 19-53-60002.
Authors thank Dr. D. Krivoruchenko and R. Boldushevskii for XRF analysis of the catalyst samples.

Conflict of Interest

The authors declare no conflict of interest.

10.1002/cctc.201901698

Keywords: Higher alcohol synthesis • Synthesis gas conversion • K-modified $MeMoS_2$ catalysts • $FeMoS_2$ • $CoMoS_2$ • $NiMoS_2$

References

1. P. Mohanty, K. Pant, S. Naik, J. Parikh, A. Hornung, J. Sahu, *Renew. Sust. Energ. Rev*. 2014, *38*, 131–153.
2. X. Hao, G. Dong, Y. Yang, Y. Xu, Y Li, *Chem. Eng. Technol.* 2007, *9*, 1157-1165.
3. L. Siwale, L. Kristo´f, T. Adam, A. Bereczky, A. Penninger, M. Mbarawa and K. Andrei, *J. Power Energy* 2013, *1*, 77–83.
4. H.T. Luk, C. Mondelli, D.C. Ferré, J.A. Stewart, J. Pérez-Ramírez, *Chem. Soc. Rev.* 2017, *46*, 1358–1426.
5. V.R. Surisetty, A.K. Dalai, J. Kozinski, *Appl. Catal., A Gen.* 2011 *404*, 1–11.
6. N. Koizumi, K. Murai, T. Ozaki, M. Yamada, *Catal. Today* 2004, *89*, 465–478.
7. P. Forzatti, E. Tronconi, I. Pasquon, *Catal. Rev.* 1991, *33*, 109-168.
8. S. Sarathy, P. Oßwald, N. Hansen, K. Kohse-Höinghaus, *Prog. Energy Combust. Sci.* 2014, *44*, 40–102.
9. K. Atsonios, M.-A. Kougioumtzis, K.D. Panopoulos, E. Kakaras, *Appl. Energy* 2015, *138*, 346-366.
10. C.-L. Song, W.-M. Zhang, Y.-Q. Pei, G.-L. Fan, G.-P. Xu, *Atmos. Environ.* 2006, *40*, 1957–1970.
11. J.M. Christensen, P.M. Mortensen, R. Trane, P.A. Jensen, A.D. Jensen, *Appl. Catal., A: Gen.* 2009, *366*, 29–43.
12. M. Feng, *Recent Patents Catal.* 2012, *1*, 13–26.
13. R. R. Stevens, patent US4882360A (1989).
14. C. B. Murchison, patent US4151190A (1979).
15. J.M. Bergthorson, M.J. Thomson, *Renew. Sustain. Energy Rev.* 2015, *42*, 1393–1417.
16. R. Magnusson, C. Nilsson, *Fuel* 2011, *90*, 1145–1154.
17. R. Quinn, T. Dahl, B. Toseland, *Appl. Catal., A: Gen.* 2004, *272*, 61–68.
18. Y. Ma, Q. Ge, W. Li, H. Xu, *Catal. Commun.* 2008, *10*, 6–10.
19. V. Kogan, N. Rozhdestvenskaya, I. Korshevets, *Appl. Catal., A* 2002, *234*, 207–219.
20. V.M. Kogan, P.A. Nikulshin, N.N. Rozhdestvenskaya, *Fuel* 2012, *100*, 2–16.
21. V. S. Dorokhov, D. I. Ishutenko, P. A. Nikul'shin, K. V. Kotsareva, E. A. Trusova, T. N. Bondarenko, O. L. Eliseev, A. L. Lapidus, N. N. Rozhdestvenskaya, V. M. Kogan, *Kin.&Catal.* 2003, *44*, 583–599.
22. E.A. Permyakov, V.S. Dorokhov, V.V. Maximov, P.A. Nikulshin, A.A. Pimerzin, V.M. Kogan, *Catal. Today* 2018, *305*, 19-27.
23. N. Koizumi, K. Murai, T. Ozaki, M. Yamada, *Catal. Today* 2004, *89*, 465–478.
24. D.A. Storm, *Top. Catal.* 1995, *2*, 91–101.
25. Y. Zhang, Y. Sun, B. Zhong, *Catal. Lett.* 2001, *76*, 249–253.
26. Z. Li, Y. Fu, J. Bao, M. Jiang, T. Hu, T. Liu, Y. Xie, *Appl. Catal., A: Gen.* 2001, *220*, 21-30.
27. J. Iranmahboob, D. Hill, H. Toghiani, *Appl. Catal., A: Gen.* 2002, *231*, 99-108.
28. V. M. Kogan, P. A. Nikulshin, *Catal. Today* 2010, *149*, 224–231.

29. V.S. Dorokhov, E.A. Permyakov, P.A. Nikulshin, V.V. Maximov, V.M. Kogan, *J. Catal.* 2016, *344*, 841-853.
30. M. Brun, A. Lallemand, J.-F. Quinson, C. Eyraud, *Thermoch. Acta* 1977, *21*, 59–88.
31. B.C. Lippens, J.H. de Boer, *J. Catal.* 1965, *4*, 319–323.
32. T. Shiota, M. Nishino, S. Kuwabara, patent US6314158B1 (2000).
33. S. Zaman, K.J. Smith, *Catal. Rev.* 2012, *54*, 41-132.
34. J.-J. Wang, J.-R. Xie, Y.-H. Huang, B.-H. Chen, G.-D. Lin, H.-B. Zhang, *Appl. Catal., A: Gen* 2013, *468*, 44– 51.
35. V.S. Dorokhov, M.A. Kamorin, N.N. Rozhdestvenskaya, V.M. Kogan, *CR Chim.* 2016, *19*, 1184-1193.
36. P.A. Nikulshin, V.A. Salnikov, A.V. Mozhaev, P.P. Minaev, V.M. Kogan, A.A. Pimerzin, *J. Catal.* 2014, *309*, 386-396.
37. F. Dumeignil, J.-F. Paul, E. W. Qian, A. Ishihara, E. Payen, T. Kabe, *Res. Chem. Intermed.* 2003, *29*, 589–607.
38. S. Helveg, J. V. Lauritsen, E. Lægsgaard, I. Stensgaard, J. K. Nørskov, B. S. Clausen, H. Topsøe, and F. Besenbacher, *Phys. Rev. Lett.* 2000, *84*, 951-954.
39. E. Krebs, B. Silvi, P. Raybaud, *Catal. Today* 2008, *130*, 160–169.
40. M. Sun, A. E. Nelson, J. Adjaye, *J. Catal.* 2005, *233*, 411–421.
41. K. Dvorak, I. Hájková, K. Havlíčková, *Adv. Mat. Res.* 2014, *1000*, 51–54.
42. V.P. Santos, B. Linden, A. Chojecki, G. Burdoni, S. Corthals, H. Shibata, G.R. Meiama, F. Kapteijn, M. Makkee, J. Gascon, *ACS Catal.* 2013, *7*, 1634-1637.
43. M.T. Claure, S.H. Chai, S. Dai, K.A. Unocic, F.M. Alamgir, P.K. Agrawal, C.W. Jones, *J. Catal.* 2015, *324*, 88-97.
44. R.B. Somoano, V. Hadek, A. Rembaum, *J. Chem. Phys.* 1973, *58*, 697.
45. J. Lu, Y. Luo, D. He, Z. Xu, S. He, D. Xie, Y. Mei, *Catal. Today* 2020, *339*, 93-104.
46. D. Ferrari, G. Budroni, L. Bisson, N.J. Rane, B.D. Dockie, J.H. Kang, S.J. Rozeveld, *Appl. Catal., A: Gen.* 2013, *462-463*, 302-309.
47. P.-Y. Prodhomme, P. Raybaud, H. Toulhoat, *J. Catal.* 2011, *280*, 178-195.
48. P. Raybaud, J. Hafner, G. Kresse, S. Kasztelan, H. Toulhoat, *J. Catal.* 2000, *190*, 128-143.
49. E. Krebs, A. Daudin, P. Raybaud, *Oil Gas Sci. Technol. – Rev. IFP* 2009, *64*, 707-718.
50. S. Cristol, J.F. Paul, E. Payen, D. Bougeard, S. Clemendot, F. Hutschka, *J. Phys. Chem.* 2002, *106*, 5659-5667.
51. M. T. Claure, L.C. Lee, J.W. Goh, L.T. Gelbaum, P.K. Agrawal, C.W. Jones, *J. of Mol. Cat. A: Chem.* 2016, *423*, 224-232.

10.1002/cctc.201901698

Table 1

Surface area and pore size analysis results

Catalyst	Specific surface area, m^2/g	Pore volume, cm^3/g	Pore diameter*, nm
Al_2O_3	171.2	0.64	4.5 and 14.9
MoS_2/Al_2O_3	114.5	0.44	3.7 and 16.1
$FeMoS_2/Al_2O_3$	131.0	0.38	3.7 and 16.0
$CoMoS_2/ Al_2O_3$	122.6	0.34	3.9 and 14.9
$NiMoS_2/ Al_2O_3$	126.9	0.37	3.8 and 17.4
$KMoS_2/ Al_2O_3$	79.3	0.35	3.9 and 15.0
$KFeMoS_2/ Al_2O_3$	69.6	0.28	3.8 and 16.0
$KCoMoS_2/ Al_2O_3$	77.4	0.28	3.7 and 15.0
$KNiMoS_2/ Al_2O_3$	85.7	0.31	3.7 and 14.5

* – bimodal pore diameter distribution.

Table 2

Results of elemental analysis of catalysts by XRF

Catalyst	Content, wt %			Ratio	
	Mo	Me	K	t**	***r****
MoS_2/Al_2O_3	12.2	—	—	—	—
$FeMoS_2/Al_2O_3$	10.9	2.1	—	—	0.25
$CoMoS_2/Al_2O_3$	11.1	2.9	—	—	0.30
$NiMoS_2/Al_2O_3$	12.8	3.1	—	—	0.28
$KMoS_2/Al_2O_3$	12.5	—	10.4	0.83	—
$KFeMoS_2/Al_2O_3$	12.8	2.1	9.3	0.62	0.22
$KCoMoS_2/Al_2O_3$	12.6	2.8	8.1	0.64	0.27
$KNiMoS_2/Al_2O_3$	14.3	3.1	10.2	0.71	0.26

*) ***r*** = Me/(Me+Mo), molar ratio
**) t=K/(Me+Mo), molar ratio

 10.1002/cctc.201901698

Table 3
Synthesis gas conversion on (K)(Me)MoS_2 catalysts and product selectivity (at 340 °C, P=5.0 MPa)

Catalyst	MoS_2	$FeMoS_2$	$CoMoS_2$	$NiMoS_2$	$KMoS_2$	$KFeMoS_2$	$KCoMoS_2$	$KNiMoS_2$
				Conversion %				
	63.0	24.1	14.6	11.5	20.2	5.6	20.4	15.1
				Selectivity, %				
CO_2	46.9	46.0	49.6	52.7	29.5	48.0	28.3	25.8
CH_4	26.8	12.9	16.6	12.1	8.1	11.2	7.8	4.6
C_2H_6	14.4	17.5	18.5	18.5	9.1	8.7	2.1	0.0
C_3H_8	7.3	10.2	6.9	8.9	0.0	0.0	0.7	0.0
C_4H_{10}	2.4	6.4	0.0	0.0	0.0	0.0	0.0	0.0
MeOH	2.2	7.0	8.5	7.8	21.7	32.2	6.5	3.8
EtOH					10.8		16.5	17.5
PrOH-1					9.9		16.2	21.2
BuOH-1					3.2		6.2	8.7
AmOH-1					0.0		2.8	3.9
PrOH-2					3.5		0.6	0.9
i-BuOH					2.5		7.6	8.0
BuOH-2					1.6		1.1	1.7
i-AmOH					0.0		3.6	3.7

Table 4.
Influence of the promotor nature on the liquid products yield (at 340 °C, P=5.0 MPa)

Catalyst	Liquid products (LP) yield, %		Effect of promoter addition on LP yield*
	K-free	K	
(K)MoS_2/Al_2O_3	1.4	10.8	7.9
(K)$FeMoS_2/Al_2O_3$	1.7	1.8	1.1
(K)$CoMoS_2/Al_2O_3$	1.2	12.5	10.1
(K)$NiMoS_2/Al_2O_3$	0.9	10.5	11.8

*) Ratio of LP yields on the K-modified catalysts to LP yields on the K-free catalysts. LP – liquid products.

10.1002/cctc.201901698

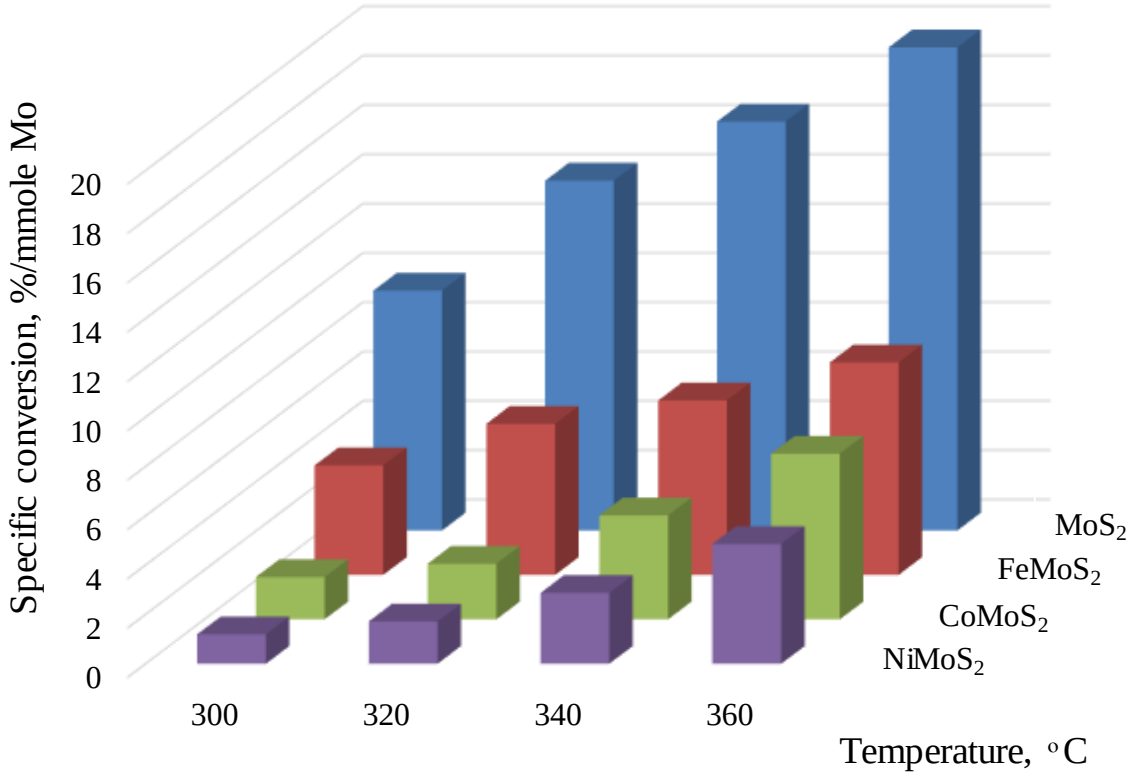

Fig. 1. Specific conversion of synthesis gas over the potassium-unmodified (Me)MoS_2 catalysts where Me = Fe, Co, Ni for different temperatures. Reaction conditions: T = 300-360 °C, P = 5.0 MPa, synthesis gas flow rate 760 $l \cdot h^{-1} \cdot (kg_{cat})^{-1}$, catalyst loading 3 grams, synthesis gas composition: $CO:H_2:Ar$ = 45:45:10.

10.1002/cctc.201901698

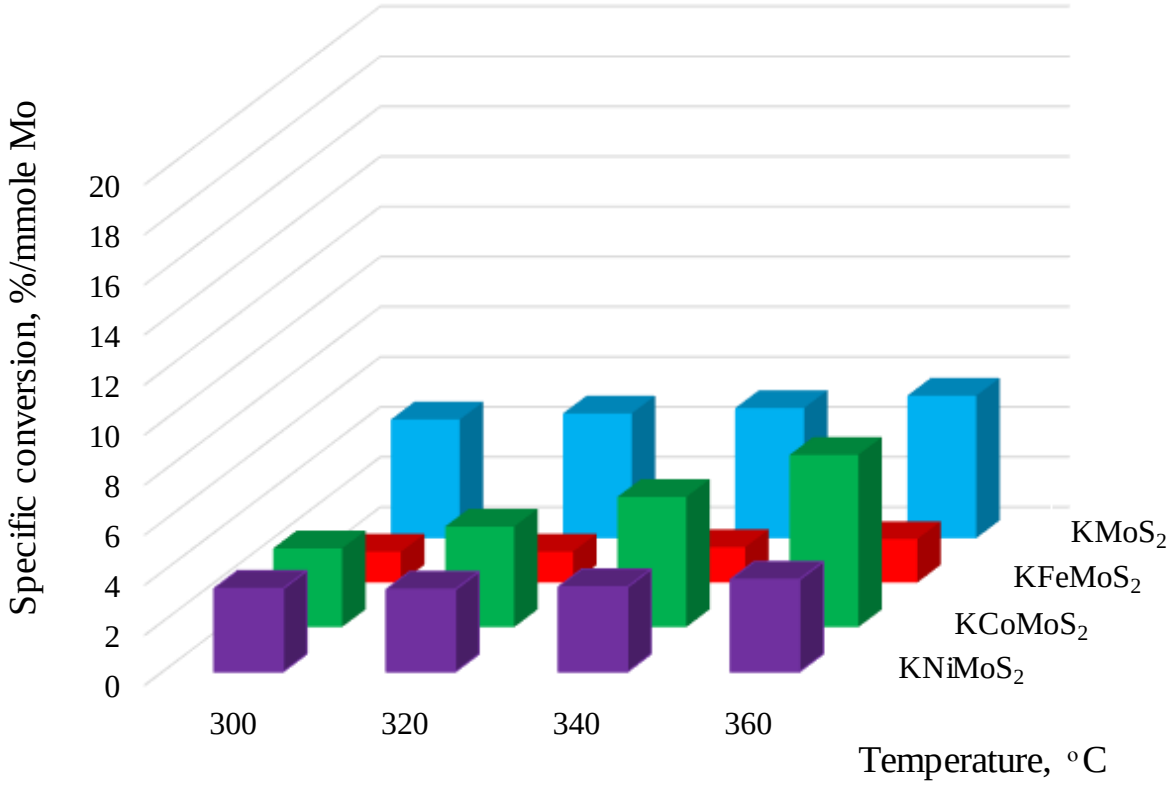

Fig. 2. Specific conversion of synthesis gas over the potassium-modified (Me)MoS_2 catalysts where Me = Fe, Co, Ni for different temperatures. For reaction conditions see Fig. 1.

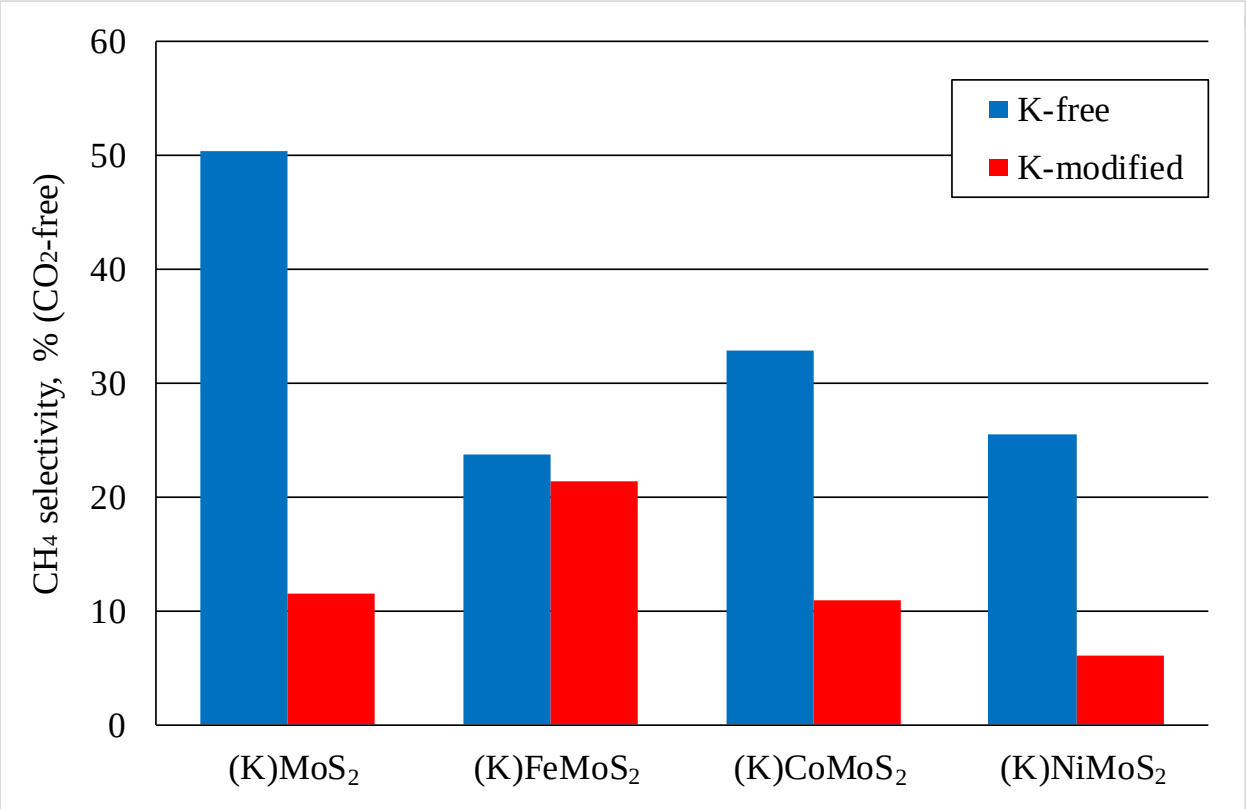

Fig. 3. Selectivity to methane at 340 °C. For detail reaction conditions see Fig. 1.

10.1002/cctc.201901698

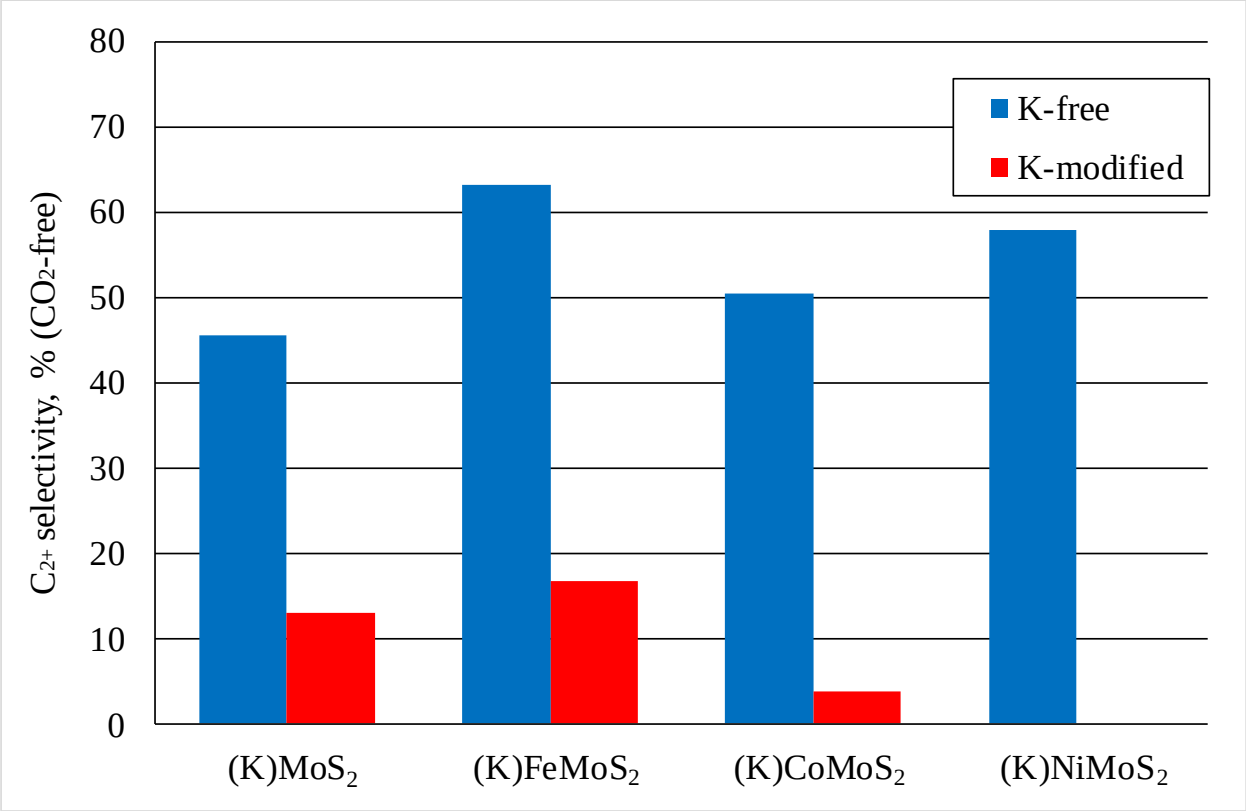

Fig. 4. Selectivity to C_{2+} hydrocarbons at 340 °C. For detail reaction conditions see Fig. 1.

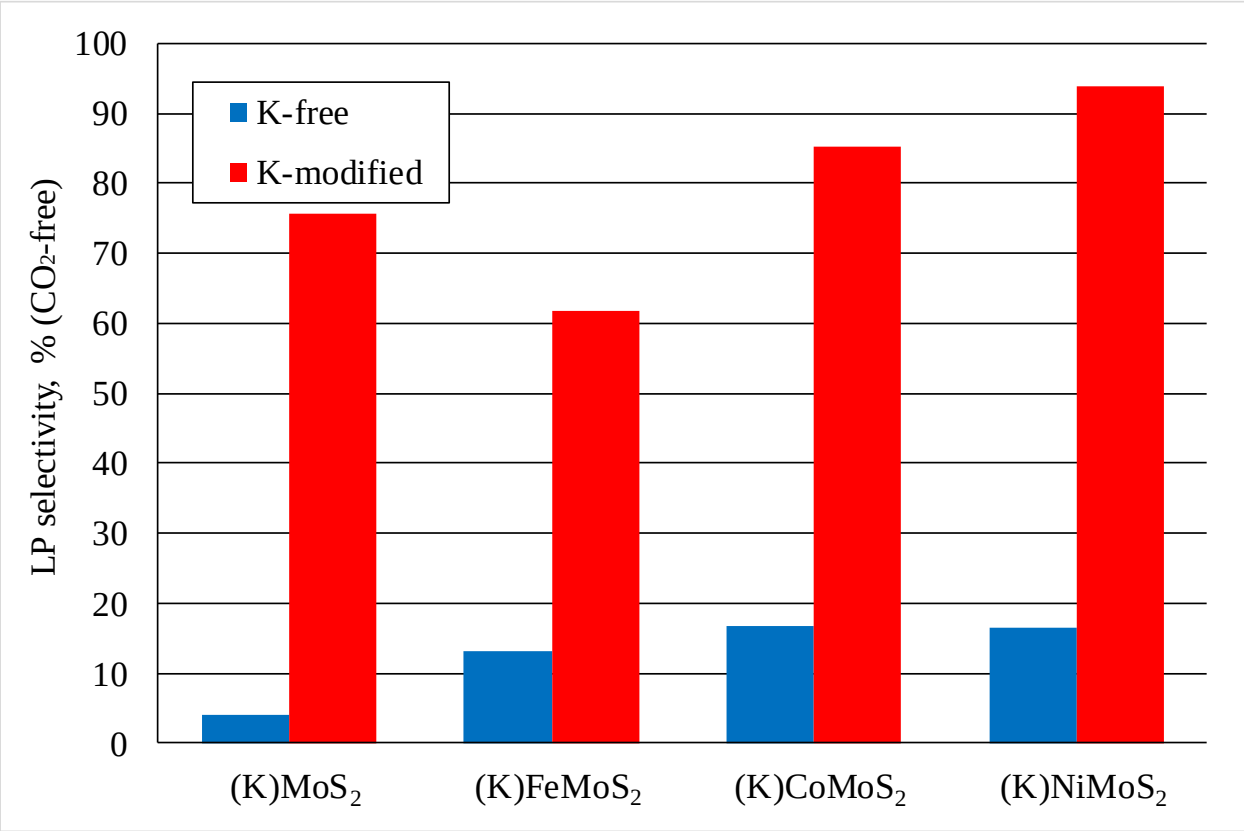

10.1002/cctc.201901698

Fig. 5. Selectivity to liquid products (LP) at 340 °C. For detail reaction conditions see Fig. 1.

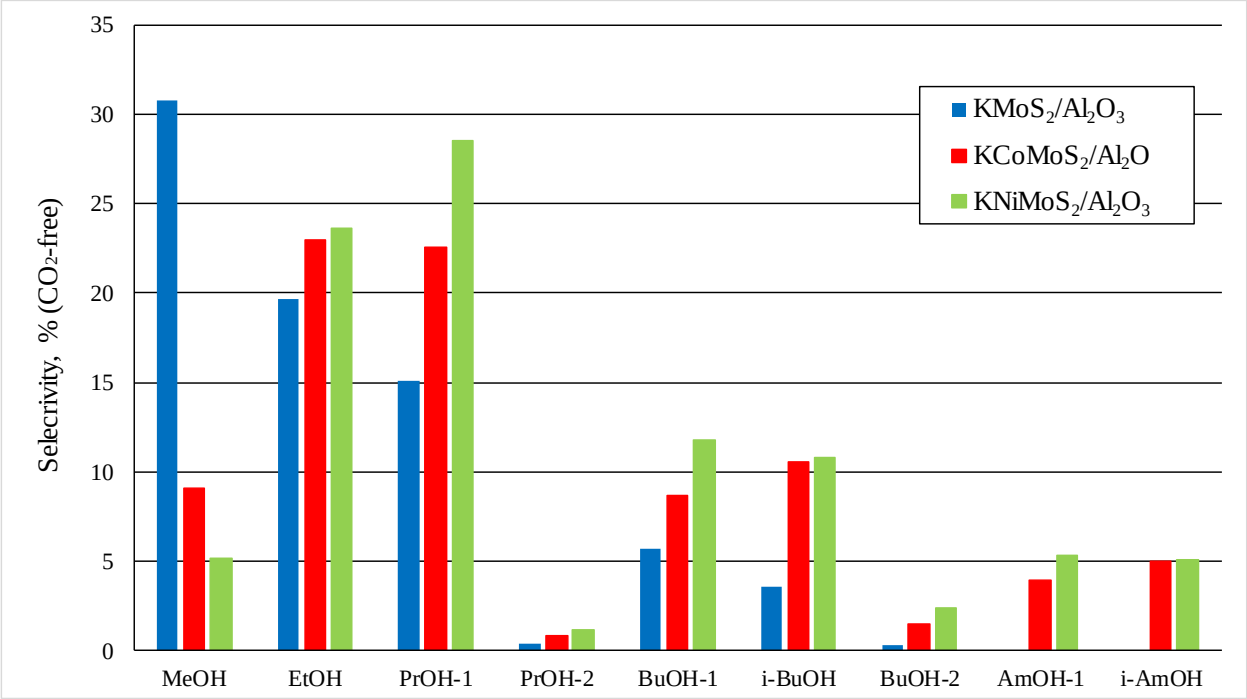

Fig. 6. Comparison of selectivity to various alcohols formed on $KMoS_2/Al_2O_3$, $KCoMoS/Al_2O_3$ and $KNiMoS/Al_2O_3$ at 340 °C. For detail reaction conditions see Fig. 1.

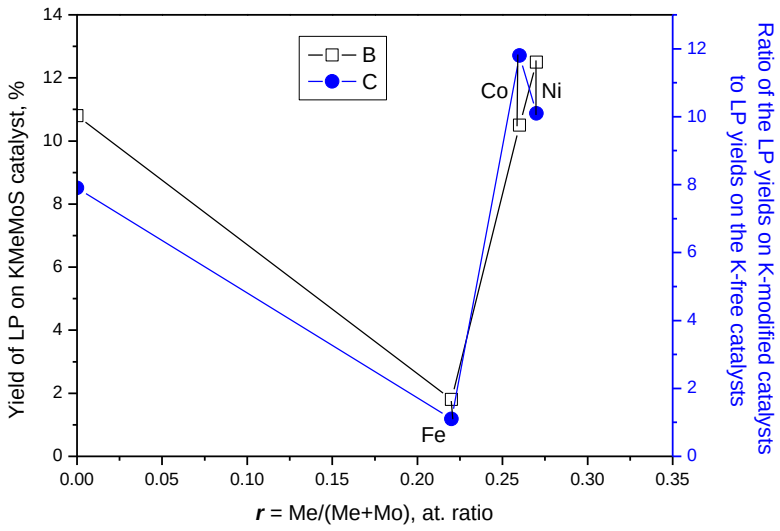

Fig. 7. Dependences of the liquid products yield and of efficiency of the potassium additive effect on the liquid products yield from the molybdenum promotion degree by iron, nickel or cobalt (***r***).

10.1002/cctc.201901698

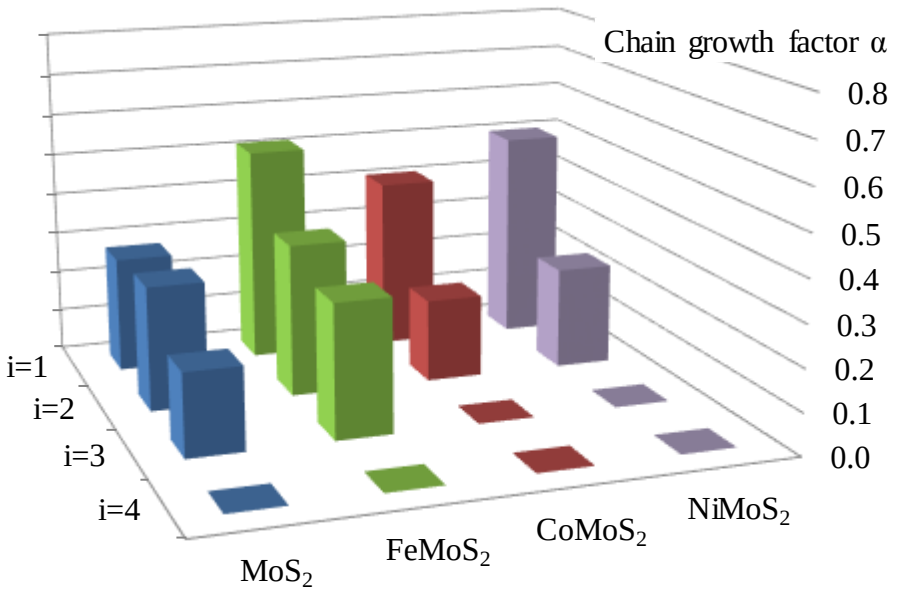

Fig. 8. Chain growth factors α_i for the steps i=1, 2, 3, 4 over the (Me)MoS_2 catalysts (Me = Fe, Co and Ni). For reaction conditions see Fig. 1.

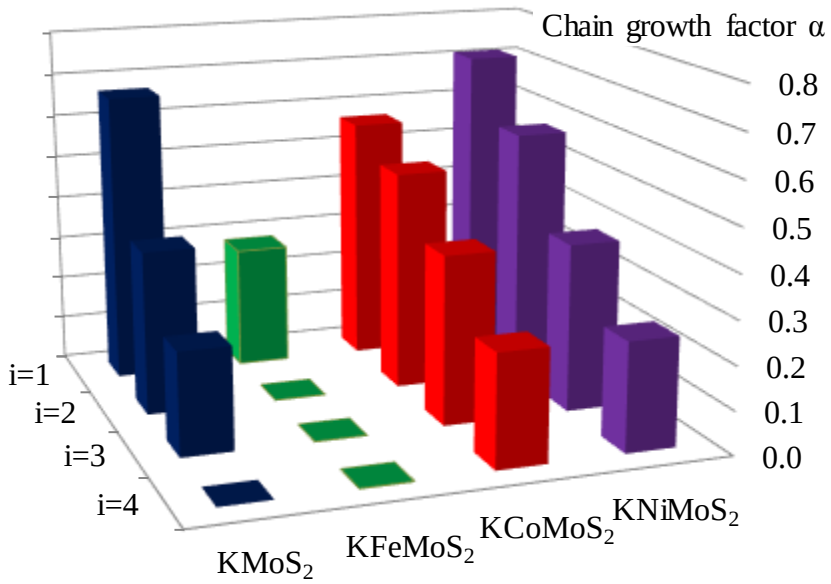

Fig. 9. Chain growth factors α_i for the steps i=1, 2, 3, 4 over the K(Me)MoS_2 catalysts (Me = Fe, Co and Ni). For reaction conditions see Fig. 1.

10.1002/cctc.201901698

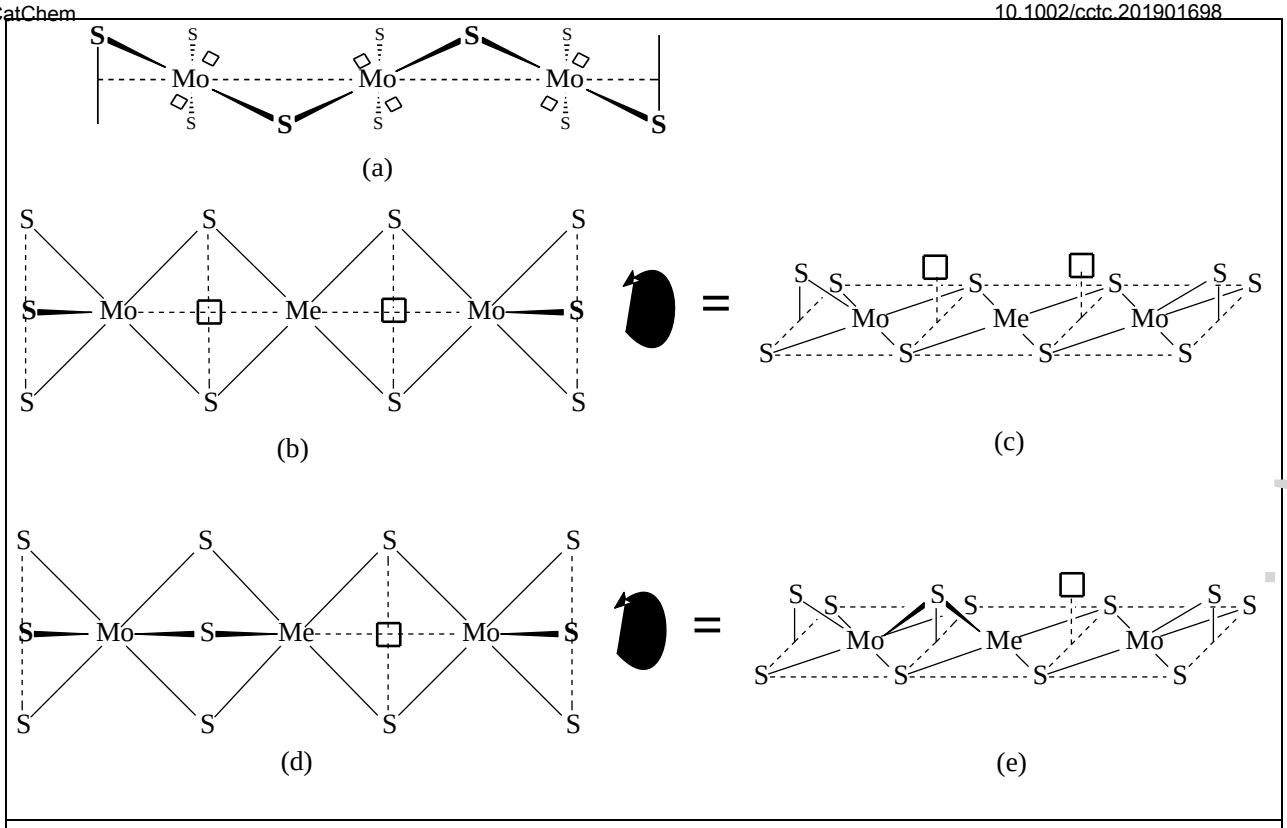

Scheme 1: Structure of the active site of the molybdenum sulfide catalyst with vacancies on molybdenum atoms. Coordination vacancies are denoted with empty squares. (a) Active site (non-promoted) on the S-edge, front view. (b) Active site (Me=Mo, Fe, Co, Ni) on the M-edge, side view. (c) Me-promoted active site (M-edge) with a double vacancy, top view. (d) Active site (Me=Mo, Fe, Co, Ni) on the M-edge, side view. (e) Me-promoted active site (M-edge) with a single vacancy, top view.

10.1002/cctc.201901698

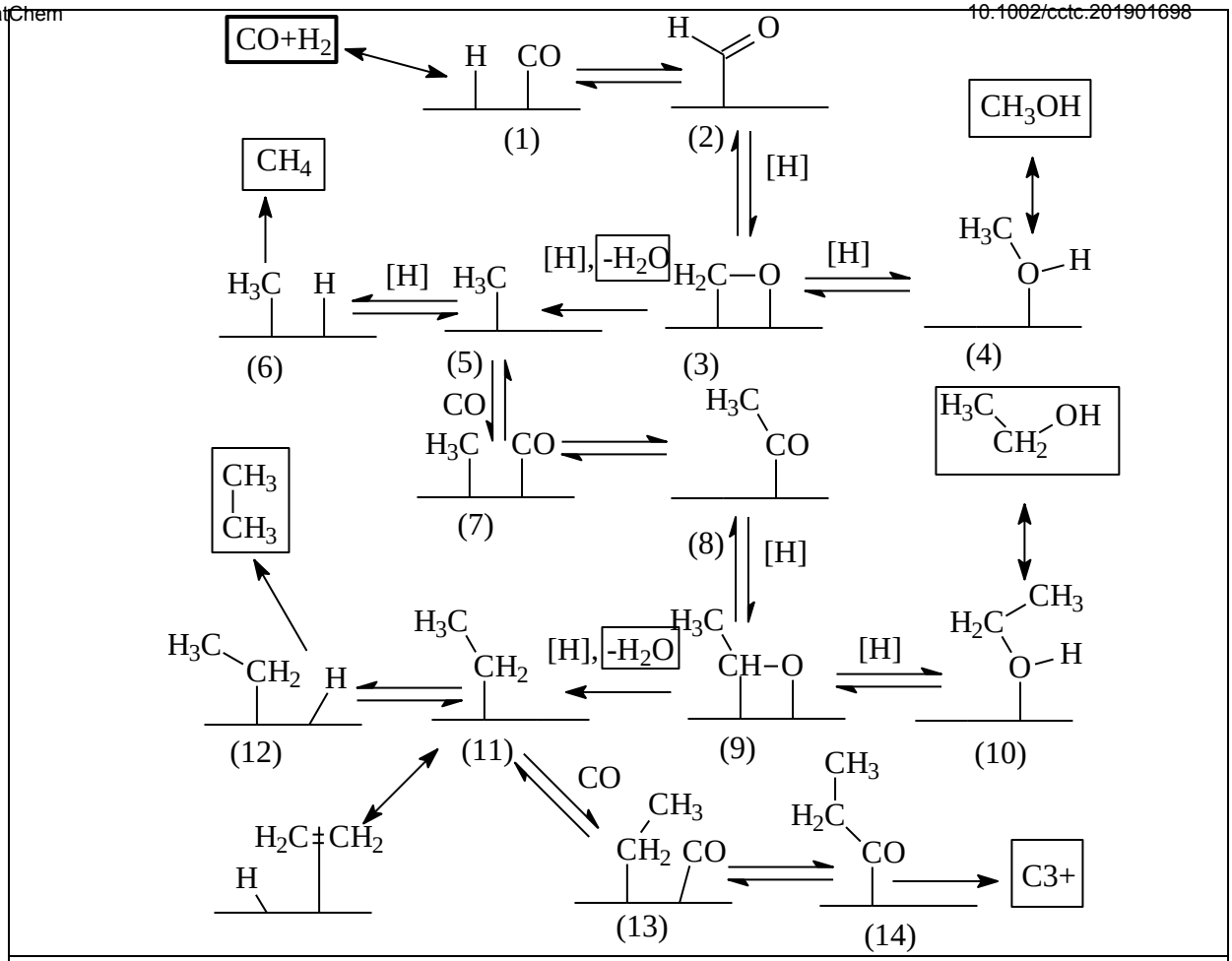

Scheme 2: Reaction pathways of synthesis gas conversion over the molybdenum sulfide catalysts.

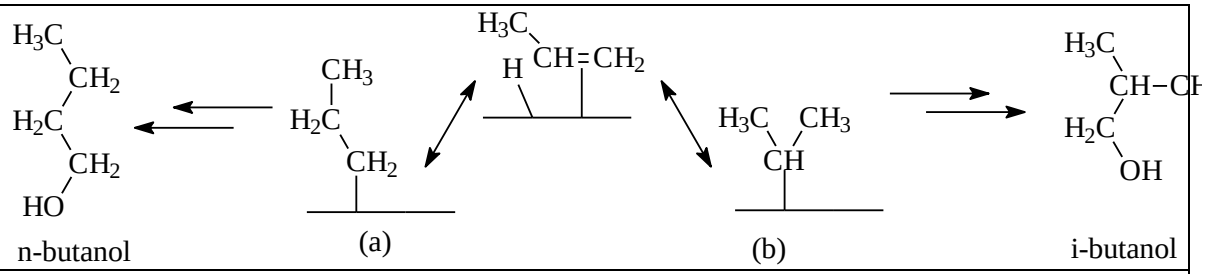

Scheme 3: Equilibrium of adsorbed alkenes and alkyl intermediates. Formation of products with the normal and branched carbon chain.

10.1002/cctc.201901698

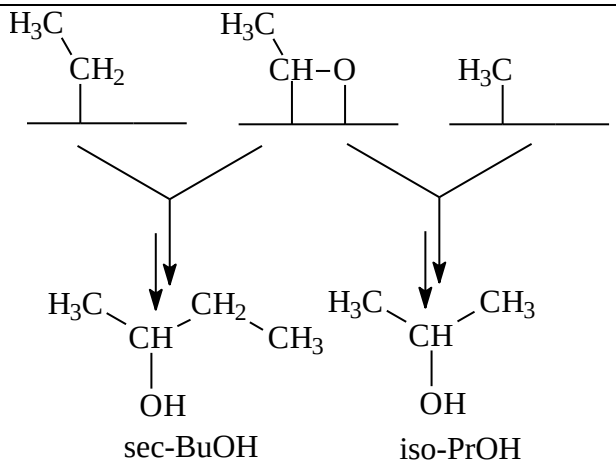

Scheme 4. Secondary alcohol formation pathway by co-elimination of aldehyde and alkyl type intermediates.